

Selected Paper

Nickel(II) Complexes of tpa Ligands with 6-Phenyl Substituents (Ph_ntpa). Structure and H_2O_2-Reactivity

Tetsuro Tano,[1] Yoshitaka Doi,[2] Masayuki Inosako,[2] Atsushi Kunishita,[1] Minoru Kubo,[3] Hirohito Ishimaru,[3] Takashi Ogura,[3] Hideki Sugimoto,[1] and Shinobu Itoh*[1,4]

[1]Department of Material and Life Science, Division of Advanced Science and Biotechnology, Graduate School of Engineering, Osaka University, 2-1 Yamada-oka, Suita, Osaka 565-0871

[2]Department of Chemistry, Graduate School of Science, Osaka City University, 3-3-138 Sugimoto, Sumiyoshi-ku, Osaka 558-8585

[3]Picobiology Institute, Graduate School of Life Science, University of Hyogo, 3-2-1 Kouto, Kamigori-cho, Ako-gun, Hyogo 678-1297

[4]Institute for Molecular Science, National Institutes of Natural Sciences, 38 Nishigo-naka, Myodaiji, Okazaki 444-8585

Received December 28, 2009; E-mail: shinobu@mls.eng.osaka-u.ac.jp

Nickel(II) complexes supported by a series of tpa {tris[(pyridin-2-yl)methyl]amine} ligand derivatives containing different numbers of phenyl substituent on the 6-position of pyridine donor group (Ph_ntpa, $n = 0$–3) have been prepared and structurally characterized. Ligand tpa and its derivatives with one or two 6-Ph substituent(s) (Ph_0tpa, Ph_1tpa, and Ph_2tpa) afforded nickel(II) complexes $\mathbf{1}^{[0]}$, $\mathbf{1}^{[1]}$, and $\mathbf{1}^{[2]}$ with a distorted octahedral geometry, whereas the ligand having three 6-Ph groups (Ph_3tpa) gave nickel(II) complex $\mathbf{1}^{[3]}$ with a five-coordinate trigonal bipyramidal structure. All the complexes exhibited a high spin ground state ($S = 1$). Reactivity of the nickel(II) complexes $\mathbf{1}^{[0]}$ and $\mathbf{1}^{[1]}$ toward H_2O_2 was very poor, whereas $\mathbf{1}^{[2]}$ and $\mathbf{1}^{[3]}$ readily gave bis(μ-oxo)dinickel(III) complexes $\mathbf{2}^{[2]}$ and $\mathbf{2}^{[3]}$, respectively, in the reaction with H_2O_2 at a low temperature. The bis(μ-oxo)dinickel(III) complexes $\mathbf{2}^{[2]}$ and $\mathbf{2}^{[3]}$ gradually decomposed to cause an aromatic hydroxylation reaction of one of the 6-Ph groups of the supporting ligands. The ligand substituent effects on the formation and decomposition processes of the bis(μ-oxo)dinickel(III) complexes are discussed based on the structures and the redox potentials of the starting nickel(II) complexes.

Tris[(pyridin-2-yl)methyl]amine (tpa), is one of the most popular tetradentate tripodal ligands in coordination chemistry.[1,2] Recently, several types of tpa derivatives have been developed in order to tune up the structure and properties of the supported complexes, where steric constraints and/or electronic effects including hydrogen-bonding interaction induced by the substituents are crucial.[1–9] Among the tpa derivatives, aryl-appended ones are a relatively new class of chelate ligands, being utilized to construct an aromatic-enriched hydrophobic environment around the secondary coordination sphere of the metal center.[1a] Notable examples are bioinorganic modeling studies using nickel and iron complexes of the aryl-appended tpa ligands carried out by Berreau et al. and Que et al.[1,4] We and others have also investigated the structure and reactivity of copper complexes supported by a series of tpa ligands with 6-phenyl substituents (Ph_ntpa, Chart 1) to find significant ligand effects on O_2 and H_2O_2 chemistry.[10–12] For instance, we have found that the reaction of H_2O_2 with $[Cu^{II}(Ph_1tpa)(CH_3CN)]^{2+}$ ($n = 1$) affords a copper(II)–hydroperoxo complex (LCu^{II}–OOH), being analogous to the reactivity of $[Cu^{II}(tpa)(CH_3CN)]^{2+}$ ($n = 0$) toward H_2O_2,[13] whereas the reaction of H_2O_2 with $[Cu^{II}(Ph_2tpa)(CH_3CN)]^{2+}$ ($n = 2$) gives a bis(μ-oxo)dicopper(III) complex.[12] Furthermore, the same treatment of $[Cu^{II}(Ph_3tpa)(CH_3CN)]^{2+}$ ($n = 3$) with H_2O_2 has been found to cause reduction of the copper(II) complex to the corresponding copper(I) complex.[12] These differences in H_2O_2-reactivity among the copper(II) complexes of Ph_ntpa have been attributed to steric as well as electronic effects of the 6-phenyl substituent(s) on the pyridine donor group(s).[12]

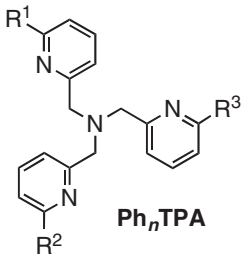

Ph$_n$TPA

$n = 0$; $R^1 = R^2 = R^3 = H$
$n = 1$; $\mathbf{R^1 = Ph}$, $R^2 = R^3 = H$
$n = 2$; $\mathbf{R^1 = R^2 = Ph}$, $R^3 = H$
$n = 3$; $\mathbf{R^1 = R^2 = R^3 = Ph}$

Chart 1. Ph_ntpa ligands.

In this study, we have extended our research of the copper–H_2O_2 chemistry to the nickel system ($\mathbf{1}^{[n]}$, $n = 0$–3) using the same series of ligands to gain further insights into the aromatic substituent effects of the tpa ligands on the structure and reactivity of the supported transition-metal complexes. Nickel/active-oxygen complexes have also attracted much recent attention due to their relevance to dioxygen activation mechanism by transition-metal complexes, and the structure

Published on the web April 29, 2010; doi:10.1246/bcsj.20090346

and reactivity of the nickel/active-oxygen complexes have frequently been discussed in connection with those of the related copper/active-oxygen complexes developed as the active site models of copper monooxygenases and copper oxidases.[5,14–18] Thus, the present study will merit considerable interest among researchers involved not only in coordination chemistry but also bioinorganic chemistry.

Experimental

Material and Apparatus. The reagents and the solvents used in this study, except the ligands and the complexes, were commercial products of the highest available purity and were further purified by standard methods, if necessary.[19] Ligands Ph_ntpa ($n = 0$–3) were synthesized according to reported procedures,[10,20–22] and $[Ni(tpa)(CH_3CN)(H_2O)](ClO_4)_2$ (**1**$^{[0]}$) and $[Ni(Ph_2tpa)(CH_3CN)(CH_3OH)](ClO_4)_2$ (**1**$^{[2]}$) were prepared according to reported methods.[22,23] FT-IR spectra were recorded on a Shimadzu FTIR-8200PC or a Jasco FTIR-4100, and UV–visible spectra were taken on a Jasco V-570 or a Hewlett Packard 8453 photo diode array spectrophotometer equipped with a Unisoku thermostated cell holder USP-203. ^{1}H NMR spectra were recorded on a JEOL FT-NMR Lambda 300WB or a JEOL FT-NMR GX-400 spectrometer. Mass spectra were recorded on a JEOL JMS-700T Tandem MS-station mass spectrometer. ESI-MS (electrospray ionization mass spectra) measurements were performed on a PE SCIEX API 150 EX. Elemental analyses were recorded with a Perkin-Elmer or Fisons instruments EA1108 Elemental Analyzer.

Cyclic voltammetric measurements were performed on an ALS-630A electrochemical analyzer in deaerated CH_3CN containing 0.10 M n-Bu_4NClO_4 as a supporting electrolyte. A Pt working electrode (BAS) was polished with BAS polishing alumina suspension and rinsed with acetone before use. The counter electrode was a platinum wire. The measured potentials were recorded with respect to an $Ag/AgNO_3$ (0.01 M) reference electrode. All electrochemical measurements were carried out in a glove box filled with Ar gas at 25 °C.

Resonance Raman scattering was dispersed by a single polychromator (Ritsu Oyo Kogaku, MC-100) and was detected by a liquid nitrogen cooled CCD detector (CCD-1024 × 256-OPEN-1LS, HORIBA Jobin Yvon). The resonance Raman measurements were carried out using a rotating NMR tube (outer diameter = 5 mm) thermostated at −90 °C by flashing cold nitrogen gas. A 135° back-scattering geometry was used.

Synthesis of Nickel(II) Complexes. **Caution!** The perchlorate salts prepared in this study are all potentially explosive and should be handled with care.

$[Ni(Ph_1tpa)(CH_3CN)_2](ClO_4)_2$ (1$^{[1]}$): To a suspension of Ph_1tpa (128.3 mg, 0.35 mmol) in CH_3CN (10 mL) was added $Ni(ClO_4)_2\cdot 6H_2O$ (128.0 mg, 0.35 mmol) in CH_3CN (15 mL), and the mixture was stirred for 30 min. The resulting pale brown solution was poured into diethyl ether (200 mL) to give the titled compound as pale brown powder in 81% (200.1 mg). IR (KBr): $\nu = 1089$ and 621 cm^{-1} (ClO_4^-). HRMS: $m/z =$ 523.0669, Calcd for $Ni(Ph_1tpa)(ClO_4)$ ($C_{24}H_{22}ClN_4NiO_4$) 523.0689. Anal. Found: C, 47.52; H, 3.96; N, 11.70%. Calcd for $[Ni(Ph_1tpa)(CH_3CN)_2](ClO_4)_2$ ($C_{28}H_{28}Cl_2N_6NiO_8$): C, 47.62; H, 4.00; N, 11.90%. UV–vis (CH_3CN): λ_{max} (ε) = 556 (30) and 936 nm (50 M^{-1} cm^{-1}). Single crystals of $[Ni(Ph_1tpa)(CH_3CN)_2](ClO_4)_2$ suitable for X-ray crystallographic analysis were obtained by slow diffusion of diethyl ether into a CH_3CN solution of the complex.

$[Ni(Ph_3tpa)(CH_3CN)](ClO_4)_2$ (1$^{[3]}$): To a suspension of Ph_3tpa (136.4 mg, 0.26 mmol) in CH_3CN (10 mL) was added $Ni(ClO_4)_2\cdot 6H_2O$ (96.2 mg, 0.26 mmol) in CH_3CN (15 mL), and the mixture was refluxed for 30 min. The resulting pale brown solution was poured into diethyl ether (200 mL) to give the titled compound as pale brown powder in 91% (194.8 mg). IR (KBr): $\nu = 1057$ and 622 cm^{-1} (ClO_4^-). HRMS: $m/z =$ 675.1309, Calcd for $Ni(Ph_3tpa)(ClO_4)$ ($C_{36}H_{30}ClN_4NiO_4$) 675.1315. Anal. Found: C, 55.78; H, 4.15; N, 8.58%. Calcd for $[Ni(Ph_3tpa)(CH_3CN)](ClO_4)_2$ ($C_{38}H_{33}Cl_2N_5NiO_8$): C, 55.84; H, 4.07; N, 8.57%. UV–vis (CH_3CN): λ_{max} (ε) = 617 (50) and 985 nm (90 M^{-1} cm^{-1}). Single crystals of $[Ni(Ph_3tpa)(CH_3CN)](ClO_4)_2$ suitable for the X-ray crystallographic analysis were obtained by slow diffusion of diethyl ether into a CH_3CN solution of the complex.

Product Analysis. $[Ni^{II}(Ph_2tpa\text{-}O)](ClO_4)$ (3$^{[2]}$): An acetone solution (50 mL) of $[Ni(Ph_2tpa)(CH_3CN)(CH_3OH)](ClO_4)_2$ (**1**$^{[2]}$) (77.3 mg, 0.1 mmol) was cooled to −78 °C using a dry ice–acetone bath. Then, 30% H_2O_2 aqueous solution (1 equiv) and Et_3N (1 equiv) were added to the solution. The resulting mixture was stirred for 1 h at −78 °C and then gradually warmed up to room temperature. After stirring for additional 30 min at room temperature, the solvent was removed under reduced pressure to give a yellow residue, to which diethyl ether (200 mL) was added. Allowing the mixture to stand for several minutes resulted in precipitation of pale yellow powder. The supernatant was then removed by decantation, and the remaining green-brown solid was washed with diethyl ether three times and dried to give **3**$^{[2]}$ in 9%. IR (KBr): $\nu = 1091$ and 703 cm^{-1} (ClO_4^-). HRMS (FAB, pos): $m/z = 515.1379$, Calcd for $Ni(Ph_3tpa\text{-}O)$ ($C_{30}H_{25}N_4NiO$) 515.1381. Anal. Found: C, 57.96; H, 4.03; N, 8.90%. Calcd for $[Ni(Ph_2tpa\text{-}O)](ClO_4)\cdot(1/2)H_2O$ ($C_{30}H_{26}ClN_4NiO_{5.5}$): C, 57.68; H, 4.20; N, 8.97%. Single crystals of $[Ni(Ph_2tpa\text{-}O)](ClO_4)\cdot CH_3CN\cdot CH_3OH$ suitable for X-ray crystallographic analysis were obtained by slow diffusion of diethyl ether into a CH_3CN/CH_3OH solution of the complex.

$[Ni^{II}(Ph_3tpa\text{-}O)](ClO_4)$ (3$^{[3]}$): An acetone solution (50 mL) of $[Ni(Ph_3tpa)(CH_3CN)](ClO_4)_2$ (**1**$^{[3]}$) (24.5 mg, 30 μmol) was cooled to −78 °C using a dry ice–acetone bath. Then, 30% H_2O_2 aqueous solution (1 equiv) and Et_3N (1 equiv) were added to the solution. The resulting mixture was stirred for 1 h at −78 °C and then gradually warmed up to room temperature. After stirring for an additional 30 min at room temperature, the solvent was removed under reduced pressure to give a brown residue, to which diethyl ether (200 mL) was added. Allowing the mixture to stand for several minutes resulted in precipitation of brown powder. The supernatant was then removed by decantation, and the remaining green-brown solid was washed with diethyl ether three times and dried to give **3**$^{[3]}$. IR (KBr): $\nu = 1081$ and 694 cm^{-1} (ClO_4^-). HRMS (FAB, pos): $m/z =$ 591.1683, Calcd for $C_{36}H_{29}N_4NiO$ 591.1694. Anal. Found: C, 59.31; H, 4.28; N, 7.50%. Calcd for $[Ni(Ph_3tpa\text{-}O)](ClO_4)\cdot 2H_2O$ ($C_{36}H_{33}ClN_4NiO_7$): C, 59.41; H, 4.57; N, 7.70%.

Hydroxylated Ligand Ph_3tpa-OH. After the reaction of **1**$^{[3]}$ and H_2O_2 described above, the reaction mixture was

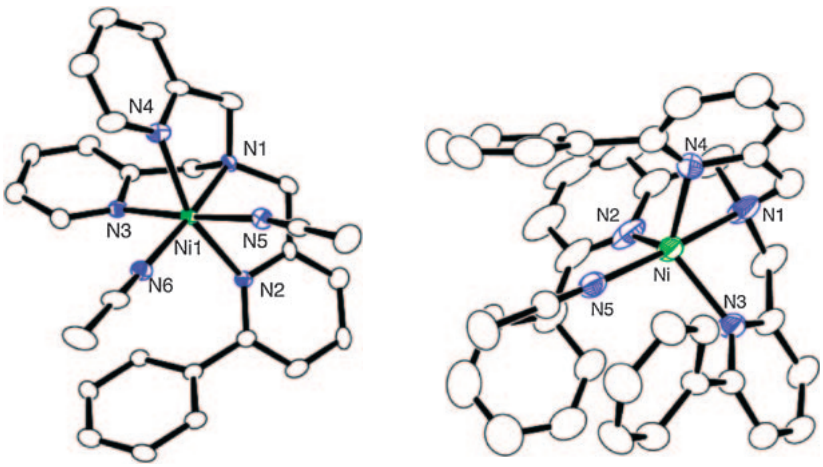

(A) (B)

Figure 1. ORTEP drawings of the cationic parts of (A) $[Ni(Ph_1tpa)(CH_3CN)_2](ClO_4)_2$ ($\mathbf{1}^{[1]}$) and (B) $[Ni(Ph_3tpa)(CH_3CN)](ClO_4)_2$ ($\mathbf{1}^{[3]}$) showing 50% probability thermal ellipsoids. The hydrogen atoms are omitted for simplicity.

acidified to pH 1 by adding concd. HCl. Removal of the solvent by evaporation gave an oily material, which was dissolved into an NH_3 aqueous solution. The aqueous solution was then extracted with diethyl ether (20 mL × 5), and the combined organic layer was dried over Na_2SO_4. After removal of Na_2SO_4 by filtration, evaporation of the solvent gave a yellow material, from which the hydroxylated ligand Ph_3tpa-OH was isolated as an oily material by silica gel column chromatography (eluent: MeOH). ^{1}H NMR (300 Hz, $CDCl_3$): δ 4.05 (4H, s, –C*H*$_2$–), 4.03 (2H, s, –C*H*$_2$–), 6.89 (1H, t, J = 7.6 Hz), 7.05 (1H, d, J = 8.2 Hz), 7.31 (1H, dt, J = 1.5 and 7.7 Hz), 7.36–7.52 (7H, m), 7.59 (2H, d, J = 11.5 Hz), 7.61 (2H, d, J = 11.1 Hz), 7.72–7.80 (5H, m), 7.99 (4H, dd, J = 1.2 and 8.3 Hz), 14.70 (1H, s, ArO*H*). HRMS (FAB, pos): m/z = 535.2493, calcd for ($C_{36}H_{30}ON_4$ + H) 535.2497.

The yield of hydroxylated product Ph_3tpa-OH was determined to be 56% based on the nickel(II) starting material by comparing an integral ratio in the ^{1}H NMR spectrum between the benzylic proton (–C*H*$_2$–) at δ 4.05 of Ph_3tpa-OH and that of the original ligand Ph_3tpa at δ 4.09.

X-ray Structure Determination. Each single crystal for $\mathbf{1}^{[1]}$, $\mathbf{1}^{[3]}$, and $\mathbf{3}^{[2]}\cdot CH_3CN\cdot CH_3OH$ was mounted on a glass-fiber. Data of X-ray diffraction were collected by a Rigaku RAXIS-RAPID imaging plate two-dimensional area detector using graphite-monochromated Mo Kα radiation (λ = 0.71069 Å). The structures were solved with SIR92.[24] All non-hydrogen atoms and hydrogen atoms except disordered atoms were refined anisotropically. Hydrogen atoms were attached ideal positions and refined using the rigid model. All the crystallographic calculations were performed by using Crystal Structure software package of the Molecular Structure Corporation[25] [Crystal Structure: Crystal Structure Analysis Package version 3.8.1, Molecular Structure Corp. and Rigaku Corp. (2005)]. Crystallographic data have been deposited with Cambridge Crystallographic Data Center: Deposition number CCDC-737436, 737437, and 737438 for compounds $\mathbf{1}^{[1]}$, $\mathbf{1}^{[3]}$, and $\mathbf{3}^{[2]}\cdot CH_3CN\cdot CH_3OH$, respectively. Copies of the data can be obtained free of charge via http://www.ccdc.cam.ac.uk/conts/retrieving.html (or from the Cambridge Crystallographic Data Centre, 12, Union Road, Cambridge, CB2 1EZ, U.K.; Fax: +44 1223 336033; e-mail: deposit@ccdc.cam.ac.uk).

Kinetic Measurements. The reaction of nickel(II) complexes with H_2O_2 was performed in a 1.0 cm path length UV–vis cell that was held in a Unisoku cryostat cell holder USP-203. After an acetone solution containing the nickel(II) complex (0.6 mM) and Et_3N (0.6 mM) was kept at a desired temperature for several minutes, H_2O_2 in acetone was injected into the cell through a septum rubber cap with use of a micro-syringe. The decomposition of the bis(μ-oxo)dinickel(III) complex was monitored by following the decrease of absorption at ca. 400 nm due to the bis(μ-oxo)dinickel(III) complex.

Results

Characterization of Nickel(II) Complexes (Starting Materials). The crystal structures of $[Ni(tpa)(CH_3CH_2CN)(H_2O)](ClO_4)_2$ ($\mathbf{1}^{[0]\prime}$ involving CH_3CH_2CN instead of CH_3CN as the co-ligand) and $[Ni(Ph_2tpa)(CH_3CN)(CH_3OH)](ClO_4)_2$ ($\mathbf{1}^{[2]}$) have already been reported in the literature.[22,23] The X-ray structures of $[Ni(Ph_1tpa)(CH_3CN)_2](ClO_4)_2$ ($\mathbf{1}^{[1]}$) and $[Ni(Ph_3tpa)(CH_3CN)](ClO_4)_2$ ($\mathbf{1}^{[3]}$) have been determined in this study as shown in Figure 1. The crystallographic data and the selected bond lengths and angles of those complexes are summarized in Tables 1 and 2, respectively.

Complex $[Ni(Ph_1tpa)(CH_3CN)_2](ClO_4)_2$ ($\mathbf{1}^{[1]}$) having one 6-phenyl substituent (6-Ph) exhibits a distorted octahedral geometry involving two acetonitrile co-ligands at *cis*-position to each other (Figure 1A). The overall structure of the nickel center resembles that of $[Ni(tpa)(CH_3CH_2CN)(H_2O)](ClO_4)_2$ ($\mathbf{1}^{[0]\prime}$) reported by Ito et al. previously, where CH_3CH_2CN and H_2O occupy the *cis*-positions instead of the two CH_3CN co-ligands in our complex $\mathbf{1}^{[1]}$.[23] However, there are notable differences in the nickel–nitrogen bond lengths between $\mathbf{1}^{[0]\prime}$ and $\mathbf{1}^{[1]}$. Namely, the bond length of Ni(1)–N(2) (2.179(3) Å) is somewhat longer than those of Ni(1)–N(3) and Ni(1)–N(4) (2.099(3) and 2.109(3) Å) in $\mathbf{1}^{[1]}$, whereas the bond lengths between the nickel ion and the three pyridine nitrogen atoms of tpa ligand in $\mathbf{1}^{[0]\prime}$ are nearly identical (2.056(8), 2.076(10), and 2.089(8) Å).[23] The elongation of the Ni(1)–N(2) bond in $\mathbf{1}^{[1]}$

Table 1. Summary of the X-ray Crystallographic Data of Complexes $\mathbf{1}^{[1]}$ and $\mathbf{1}^{[3]}$

Complex	$\mathbf{1}^{[1]}$	$\mathbf{1}^{[3]}$
Formula	$C_{28}H_{28}Cl_2N_6NiO_8$	$C_{38}H_{33}N_5NiCl_2O_8$
Formula weight	706.17	817.31
Crystal system	monoclinic	triclinic
Space group	$P2_1/n$ (#14)	$P\bar{1}$ (#2)
a/Å	10.1684(7)	10.931(7)
b/Å	10.7955(8)	13.350(11)
c/Å	28.3903(18)	13.404(11)
α/°	—	91.06(3)
β/°	89.801(5)	94.19(3)
γ/°	—	111.94(2)
V/Å^3	3116.5(4)	1807.4(23)
Z	4	2
F(000)	1456.00	844.00
D_{calcd}/g cm^{-3}	1.505	1.502
T/K	100	153
Crystal size/mm^3	0.23 × 0.20 × 0.20	0.40 × 0.30 × 0.20
μ (Mo Kα)/cm^{-1}	8.524	7.458
$2\theta_{max}$/°	55.0	55.0
No. of reflns measd	15551	17833
No. of reflns obsd	6343(All reflections)	8817($[I > 2.00\sigma(I)]$)
No. of variables	407	520
R[a)]	0.0800	0.0558
R_w[b)]	0.2003	0.0780
GOF	0.925	0.982

a) $R = \Sigma||F_o| - |F_c||/\Sigma|F_o|$. b) $R_w = [\Sigma w(|F_o| - |F_c|)^2/\Sigma wF_o^2]^{1/2}$.

could be attributed to steric repulsion between the 6-Ph substituent on the pyridine donor group and the bound CH_3CN co-ligands.

$[Ni(Ph_2tpa)(CH_3CN)(CH_3OH)](ClO_4)_2$ ($\mathbf{1}^{[2]}$), reported by Berreau et al., also exhibits a distorted octahedral geometry, where the bond lengths between the nickel ion and the nitrogen atoms of the pyridine donor groups having 6-Ph (2.218(5) and 2.200(5) Å) are also longer than that between the metal ion and the nitrogen atom of the pyridine ring without 6-Ph (2.065(4) Å).[22]

Interestingly, $[Ni(Ph_3tpa)(CH_3CN)](ClO_4)_2$ ($\mathbf{1}^{[3]}$) shows a five-coordinate trigonal bipyramidal structure with the three pyridine nitrogen atoms N(2), N(3), and N(4) occupying the basal plane and the *tert*-amine nitrogen N(1) and that of the CH_3CN co-ligand N(5) at the axial positions as shown in Figure 1B. Thus, the structure of $\mathbf{1}^{[3]}$ is exceptional among the four nickel(II) complexes $\mathbf{1}^{[n]}$ ($n = 0$–3) with respect to the coordination number (five vs. six) and geometry (trigonal bipyramidal vs. octahedral). This could be attributed to the steric restriction induced by the three 6-Ph groups in $\mathbf{1}^{[3]}$.

Berreau et al. reported the ^{1}H NMR spectrum of $\mathbf{1}^{[2]}$ with a high spin ground state ($S = 1$) in CD_3CN which exhibited several isotropically shifted resonances spread over a chemical shift range of ca. 60 ppm.[26] Other nickel(II) complexes $\mathbf{1}^{[0]}$, $\mathbf{1}^{[1]}$, and $\mathbf{1}^{[3]}$ also exhibit similar ^{1}H NMR spectra as shown in Figures S1–S3, clearly indicating that they also have a high-spin ground state ($S = 1$) as in the case of $\mathbf{1}^{[2]}$.

Redox potential of the complexes is a good indicator of the electronic effects of the ligand substituents (6-Ph).[12] The

Table 2. Selected Bond Lengths/Å and Angles/° of Complexes $\mathbf{1}^{[1]}$ and $\mathbf{1}^{[3]}$

Complex $\mathbf{1}^{[1]}$			
Ni(1)–N(1)	2.093(3)	Ni(1)–N(2)	2.179(3)
Ni(1)–N(3)	2.099(3)	Ni(1)–N(4)	2.109(3)
Ni(1)–N(5)	2.082(5)	Ni(1)–N(6)	2.039(4)
N(1)–Ni(1)–N(2)	78.57(14)	N(1)–Ni(1)–N(3)	82.62(14)
N(1)–Ni(1)–N(4)	81.72(15)	N(1)–Ni(1)–N(5)	97.33(15)
N(1)–Ni(1)–N(6)	174.84(15)	N(2)–Ni(1)–N(3)	101.11(14)
N(2)–Ni(1)–N(4)	159.02(15)	N(2)–Ni(1)–N(5)	83.44(14)
N(2)–Ni(1)–N(6)	103.46(15)	N(3)–Ni(1)–N(4)	83.28(15)
N(3)–Ni(1)–N(5)	175.32(14)	N(3)–Ni(1)–N(6)	92.31(15)
N(4)–Ni(1)–N(5)	92.08(15)	N(4)–Ni(1)–N(6)	96.79(15)
N(5)–Ni(1)–N(6)	87.65(15)		
Complex $\mathbf{1}^{[3]}$			
Ni(1)–N(1)	2.043(3)	Ni(1)–N(2)	2.062(3)
Ni(1)–N(3)	2.090(3)	Ni(1)–N(4)	2.056(3)
Ni(1)–N(5)	1.995(3)		
N(1)–Ni(1)–N(2)	80.49(16)	N(1)–Ni(1)–N(3)	78.85(14)
N(1)–Ni(1)–N(4)	80.30(14)	N(1)–Ni(1)–N(5)	177.16(16)
N(2)–Ni(1)–N(3)	117.62(14)	N(2)–Ni(1)–N(4)	113.37(14)
N(2)–Ni(1)–N(5)	97.81(14)	N(3)–Ni(1)–N(4)	119.89(15)
N(3)–Ni(1)–N(5)	100.05(12)	N(4)–Ni(1)–N(5)	102.49(12)

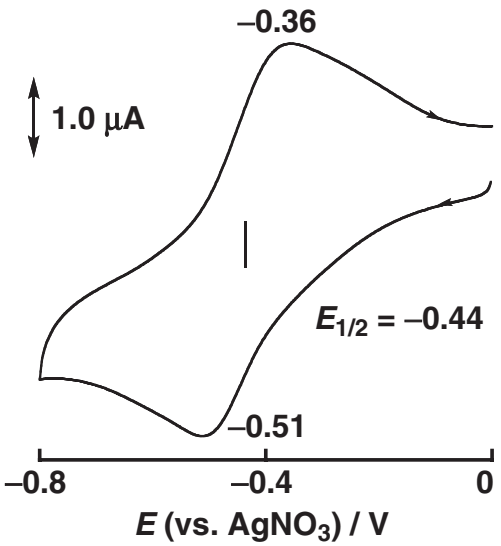

Figure 2. Cyclic voltammogram of $\mathbf{1}^{[0]}$ (4 mM) in deaerated acetone containing 0.01 M n-Bu_4NClO_4 at 25 °C; working electrode Pt, counter electrode Pt, reference electrode Ag/0.01 M $AgNO_3$ in CH_3CN, scan rate 0.05 V s^{-1}.

nickel(II) complexes $\mathbf{1}^{[n]}$ exhibit a pair of redox peaks corresponding to the reduction and re-oxidation of nickel(II). Figure 2 shows a cyclic voltammogram (CV) of $\mathbf{1}^{[0]}$ as a typical example and those of other complexes are presented in Supporting Information (Figures S4–S6). The $E_{1/2} = (E^{red}_p + E^{ox}_p)/2$ thus obtained are listed in Table 3.

Apparently, the $E_{1/2}$ values of $\mathbf{1}^{[0]}$, $\mathbf{1}^{[1]}$, and $\mathbf{1}^{[2]}$, which have a similar octahedral structure, are nearly identical (−0.41– −0.43 V vs. Ag/0.01 M $AgNO_3$), whereas that of $\mathbf{1}^{[3]}$

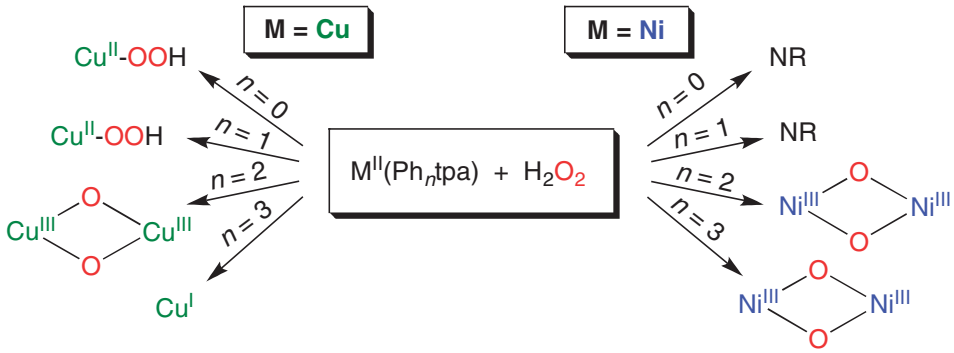

Scheme 1. H_2O_2 reactivity of Ni^{II} and Cu^{II} complexes of Ph_ntpa.

Table 3. CV Data for the Electrochemical Redox Reaction of $\mathbf{1}^{[n]}$ in Acetonitrile (V vs. Ag/0.01M $AgNO_3$)

Complex	E^{red}_p/V	E^{ox}_p/V	ΔE_p/V	$E_{1/2}$/V
$\mathbf{1}^{[0]}$	−0.51	−0.36	0.15	−0.44
$\mathbf{1}^{[1]}$	−0.52	−0.29	0.23	−0.41
$\mathbf{1}^{[2]}$	−0.61	−0.25	0.36	−0.43
$\mathbf{1}^{[3]}$	−0.87	−0.76	0.11	−0.82

showing the trigonal-bipyramidal geometry is significantly negative (−0.82 V). Such a large difference in $E_{1/2}$ between the former three and the later one could be attributed to the different geometry of the complexes (octahedral vs. trigonal bipyramidal).

H_2O_2 Reactivity. Reaction of the nickel(II) complexes and H_2O_2 was then examined to see the reactivity difference between the copper(II) complexes and the nickel(II) complexes supported by the same series of the supporting ligands. As stated in the introduction, the copper(II) complexes of Ph_ntpa exhibit quite different reactivity toward H_2O_2 depending on the number of 6-Ph substituent on the pyridine donor group.[12,13] Namely, $[Cu^{II}(tpa)(CH_3CN)]^{2+}$ ($n = 0$) and $[Cu^{II}(Ph_1tpa)(CH_3CN)]^{2+}$ ($n = 1$) provided a copper(II) hydroperoxo complex LCu^{II}–OOH, whereas $[Cu^{II}(Ph_2tpa)(CH_3CN)]^{2+}$ ($n = 2$) gave a bis(μ-oxo)dicopper(III) complex under the same reaction conditions. On the other hand, $[Cu^{II}(Ph_3tpa)(CH_3CN)]^{2+}$ ($n = 3$) was reduced to the copper(I) complex in the reaction with H_2O_2 under the same experimental conditions (Scheme 1, left).

Treatment of $\mathbf{1}^{[0]}$ and $\mathbf{1}^{[1]}$ (0.6 mM) supported by tpa and Ph_1tpa ($n = 0$ and 1), respectively, with H_2O_2 (0.6–12.0 mM) in the presence of Et_3N (3.0 mM) as a base in acetone or in acetonitrile at a temperature range from −40 °C to room temperature caused almost no change of the UV–vis spectrum. Thus, it can be concluded that the H_2O_2-reactivity of the nickel(II) complexes of these two ligands is significantly lower than that of the copper(II) complexes supported by the same ligands, which readily provided LCu^{II}–OOH at a low temperature (−80 °C).[12,13]

On the other hand, treatment of $\mathbf{1}^{[2]}$ (0.6 mM, $n = 2$) with H_2O_2 (3.0 mM) in acetone at −70 °C in the presence of Et_3N (0.6 mM) resulted in color change from pale purple to brown. In Figure 3 is shown a spectral change for the reaction, where an absorption band at 398 nm readily appeared. The final

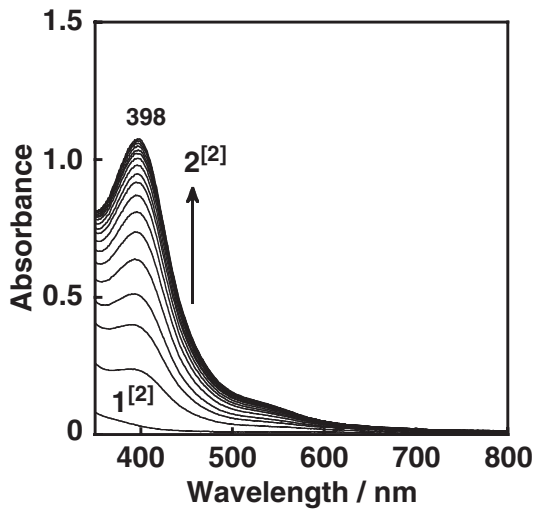

Figure 3. Spectral change observed upon addition of H_2O_2 (3.0 mM) to an acetone solution of $\mathbf{1}^{[2]}$ (0.6 mM) in the presence of triethylamine (0.6 mM) at −70 °C generating bis(μ-oxo)dinickel(III) complex $\mathbf{2}^{[2]}$.

spectrum is very close to those of the reported bis(μ-oxo)dinickel(III) complexes.[14] Furthermore, the resonance Raman spectrum of the reaction solution shown in Figure 4 exhibits a Raman band at 614 cm^{-1} with $H_2{}^{16}O_2$ (solid line spectrum) which is ascribable to the Ni_2O_2 core vibration.[27] These spectroscopic features (UV–vis and resonance Raman) clearly suggest that the generated brown species is a bis(μ-oxo)dinickel(III) complex $\mathbf{2}^{[2]}$ as shown in Scheme 2. Although the detailed structure of $\mathbf{2}^{[2]}$ is not clear at present, each metal center of the Ni_2O_2 core may have a square-planar geometry with weakly coordinated pyridine donor groups having 6-Ph in the axial positions as illustrated in Scheme 2. A similar structure was reported by Suzuki et al. for the bis(μ-oxo)-dinickel(III) complex supported by Me_2tpa (bis[(6-methylpyridin-2-yl)methyl][(pyridin-2-yl)methyl]amine).[14c] In an isotope labeling experiment using $H_2{}^{18}O_2$, a small resonance Raman band appeared at ca. 580 cm^{-1} (marked by asterisk in Figure 4), but most of the resonance Raman band at 614 cm^{-1} remained unchanged (dotted line spectrum). This may be due to rapid exchange of the oxygen atoms of the oxo groups of $\mathbf{2}^{[2]}$ with that of water.[28] A similar phenomena (no isotope shift in the Raman measurement) was also reported in other bis(μ-oxo)dinickel(III) systems.[14a,14c]

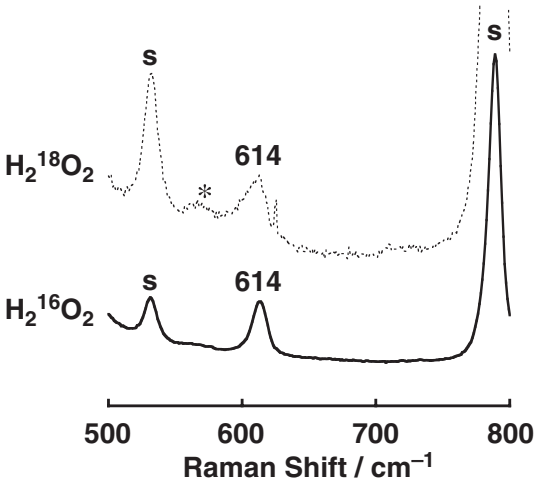

Figure 4. Resonance Raman spectra of the reaction solution of $\mathbf{1}^{[2]}$ with $H_2{}^{16}O_2$ (solid line) and with $H_2{}^{18}O_2$ (dotted line) obtained with an excitation at $\lambda_{ex} = 406.7$ nm in acetone at −90 °C: "s" denotes a solvent Raman band.

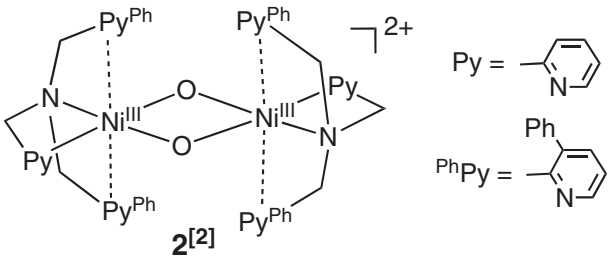

Scheme 2. Presumed structure of bis(μ-oxo)dinickel(III) complex $\mathbf{2}^{[2]}$.

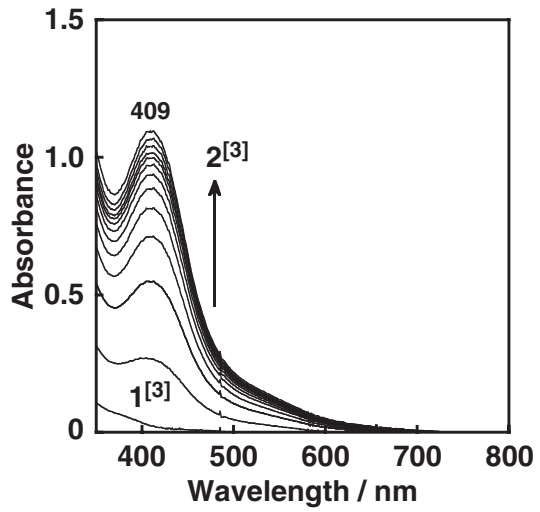

Figure 5. Spectral change observed upon addition of H_2O_2 (3.0 mM) to an acetone solution of $\mathbf{1}^{[3]}$ (0.6 mM) in the presence of triethylamine (0.6 mM) at −70 °C generating bis(μ-oxo)dinickel(III) complex $\mathbf{2}^{[3]}$.

The reaction of $\mathbf{1}^{[3]}$ and H_2O_2 under the same experimental conditions provided a similar UV–vis spectrum ($\lambda_{max} =$ 409 nm) as shown in Figure 5, and a resonance Raman band

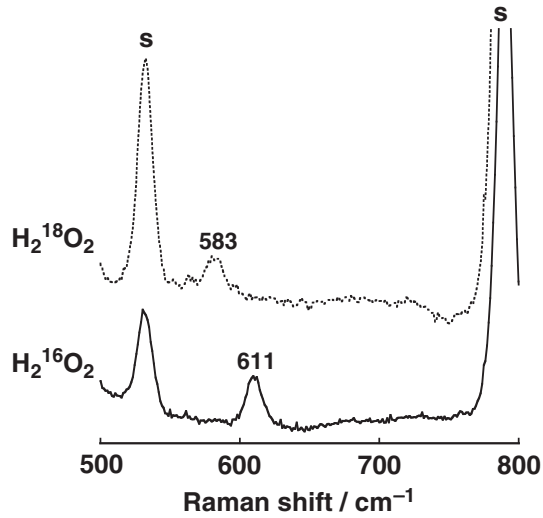

Figure 6. Resonance Raman spectra of $\mathbf{2}^{[3]}$ generated by the reaction of $\mathbf{1}^{[3]}$ with $H_2{}^{16}O_2$ (solid line) and with $H_2{}^{18}O_2$ (dotted line) obtained with an excitation at $\lambda_{ex} = 406.7$ nm in acetone at −90 °C: "s" denotes a solvent Raman band.

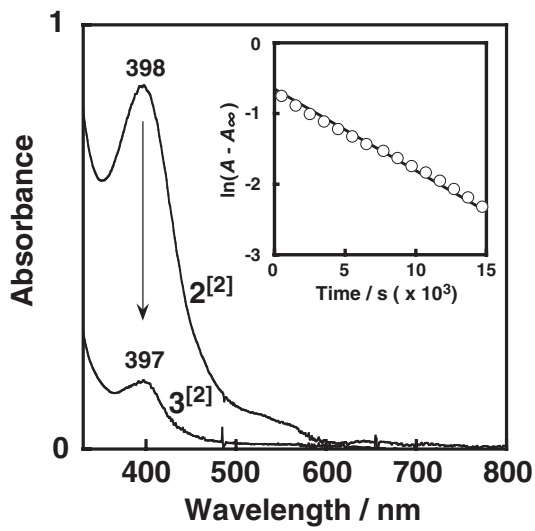

Figure 7. Spectral change for the conversion of $\mathbf{2}^{[2]}$ (0.6 mM) to $\mathbf{3}^{[2]}$ in acetone at −40 °C.

at 611 cm^{-1} (Figure 6, solid line spectrum). In this case, $\mathbf{2}^{[3]}$ exhibited an isotope shift of the Raman band at 611 to 583 cm^{-1} upon ^{18}O-substitution using $H_2{}^{18}O_2$ (dotted line). The observed isotope shift of $\Delta\nu = 28$ cm^{-1} is in the range of those of the bis(μ-oxo) dimetallic complexes.[27] These spectroscopic features suggest that complex $\mathbf{2}^{[3]}$ has a similar bis(μ-oxo)-dinickel(III) core. Enhanced steric bulkiness of Ph_3tpa by the additional 6-Ph groups in the equatorial position may protect the Ni_2O_2 core from attack by water, thus preventing the oxygen exchange reaction between the oxo groups and H_2O.

Decomposition Product. Bis(μ-oxo)dinickel(III) complex $\mathbf{2}^{[2]}$ was relatively stable at a low temperature (−70 °C), but gradually decomposed at a higher temperature (−40 °C) obeying first-order kinetics (Figure 7, $k_{dec} = 1.1 \times 10^{-4}$ s^{-1}). In the UV–vis spectrum of the final reaction mixture shown in

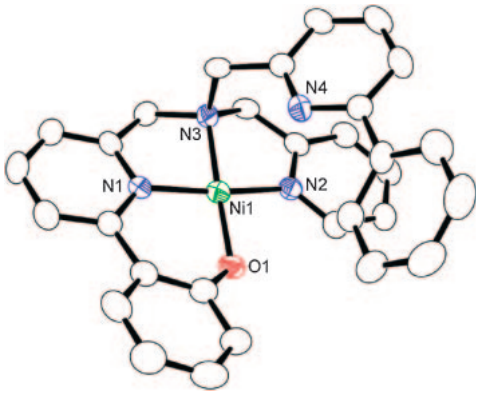

Figure 8. ORTEP drawing of the cationic part of $\mathbf{3}^{[2]}\cdot CH_3CN\cdot CH_3OH$ showing 50% probability thermal ellipsoids. The hydrogen atoms are omitted for simplicity.

Table 4. Summary of the X-ray Crystallographic Data of Complex $\mathbf{3}^{[2]}\cdot CH_3CN\cdot CH_3OH$

Compound	$\mathbf{3}^{[2]}\cdot CH_3CN\cdot CH_3OH$
Formula	$C_{33}H_{32}N_5NiClO_6$
Formula weight	688.80
Crystal system	monoclinic
Space group	$P2_1/a$ (#14)
a/Å	11.820(9)
b/Å	20.585(14)
c/Å	12.922(12)
α/°	90
β/°	99.54(3)
γ/°	90
V/Å^3	3100(4)
Z	4
F(000)	1432.00
D_{calcd}/g cm^{-3}	1.475
T/K	153
Crystal size/mm^3	0.40 × 0.30 × 0.20
μ (Mo Kα)/cm^{-1}	7.663
$2\theta_{max}$/°	55.0
No. of reflns measd	28864
No. of reflns obsd	5051($[I > 0.40\sigma(I)]$)
No. of variables	447
R[a)]	0.0429
R_w[b)]	0.0476
GOF	0.979

a) $R = \Sigma||F_o| - |F_c||/\Sigma|F_o|$. b) $R_w = [\Sigma w(|F_o| - |F_c|)^2/\Sigma wF_o^2]^{1/2}$.

Figure 7, there is a small absorption band at 397 nm which is due to the ligand hydroxylated product as described below (the smaller absorbance is due to the lower yield of the hydroxylated product, see below).

The hydroxylated complex was isolated as a minor product (9% yield determined by ^{1}H NMR of the organic product mixture after work-up, ca. 90% of original ligand was recovered) from the final reaction mixture in a preparative scale, and its structure was determined by X-ray crystallographic analysis as indicated in Figure 8 (the crystallographic data and the selected bond lengths and angles of those

Table 5. Selected Bond Lengths/Å and Angles/° of Complex $\mathbf{3}^{[2]}\cdot CH_3CN\cdot CH_3OH$

Complex $\mathbf{3}^{[2]}\cdot CH_3CN\cdot CH_3OH$			
Ni(1)–N(1)	1.862(2)	Ni(1)–N(2)	1.886(3)
Ni(1)–N(3)	1.902(3)	Ni(1)–O(1)	1.817(2)
N(1)–Ni(1)–N(2)	170.82(16)	N(1)–Ni(1)–N(3)	86.35(14)
N(2)–Ni(1)–N(3)	85.74(14)	O(1)–Ni(1)–N(1)	95.22(13)
O(1)–Ni(1)–N(2)	92.80(13)	O(1)–Ni(1)–N(3)	177.96(12)

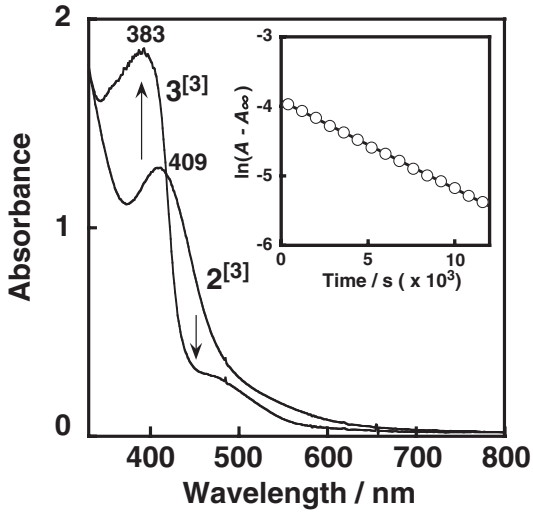

Figure 9. Spectral change for the conversion of $\mathbf{2}^{[3]}$ (0.6 mM) to $\mathbf{3}^{[3]}$ in acetone at −40 °C.

complexes are summarized in Tables 4 and 5, respectively). As clearly seen, one of the 6-Ph groups is hydroxylated at its *o*-position to give a mononuclear Ni^{II}–phenolate complex $\mathbf{3}^{[2]}$, where the nickel center exhibited a distorted square-planar structure with a N_3O donor set provided by the modified ligand ($L^{[2]}$–OH).

Bis(μ-oxo)dinickel(III) product $\mathbf{2}^{[3]}$ decomposed more readily, also obeying first-order kinetics ($k_{dec} = 1.3 \times 10^{-3}$ s^{-1}) (Figure 9), and the ligand hydroxylated product having an absorption band at 383 nm was produced as a major product (56% yield determined by ^{1}H NMR of the organic product mixture after work-up, ca. 40% of original ligand was recovered). Although the mechanistic details have yet to be examined, the aromatic hydroxylation may proceed via electrophilic aromatic substitution as previously demonstrated for the Ni^{II}/H_2O_2 systems.[14b,29,30]

Discussion

In order to get insights into the substituent effects on the structure and reactivity of the tpa-complexes, nickel(II) complexes supported by a series of tpa ligands containing different number of 6-Ph have been prepared and structurally characterized. Ph_ntpa with $n = 0$, 1, and 2 afforded the nickel(II) complexes $\mathbf{1}^{[0]}$, $\mathbf{1}^{[1]}$, and $\mathbf{1}^{[2]}$ with a distorted octahedral geometry, whereas Ph_3tpa gave a nickel(II) complex with a trigonal-bipyramidal structure. The sterically bulkier ligand Ph_3tpa may prevent the complex from having a six-coordinate geometry with two additional external co-ligands, thus provid-

ing the complex with a five-coordinate trigonal-bipyramidal structure with only one external ligand.

With respect to the reactivity, nickel(II) complexes $\mathbf{1}^{[0]}$ and $\mathbf{1}^{[1]}$ hardly reacted with H_2O_2 (Scheme 1, right). The poor reactivity of the nickel(II) complexes of tpa and Ph_1tpa toward H_2O_2 is significantly different from the high H_2O_2-reactivity of the copper(II) complexes of the same ligands, which afford LCu^{II}–OOH complexes (Scheme 1, left).[12,13] Such a reactivity difference between the nickel(II) and copper(II) complexes could be attributed to a lower Lewis acidity of nickel(II) as compared with copper(II). Namely, Lewis acidity of nickel(II) may not be strong enough to stabilize the hydroperoxide adduct. In fact, there have been few examples of mononuclear nickel(II)–hydroperoxo complexes LNi^{II}–OOH, whereas many examples of LCu^{II}–OOH complexes have so far been reported.[31]

On the other hand, $\mathbf{1}^{[2]}$ and $\mathbf{1}^{[3]}$ supported by Ph_2tpa and Ph_3tpa, respectively, provided the bis(μ-oxo)dinickel(III) complex $\mathbf{2}^{[2]}$ and $\mathbf{2}^{[3]}$ in the reaction with H_2O_2 at low temperature (Scheme 1, right). Increasing the number of 6-Ph groups of the ligands may cause a decrease of electron-donor ability of pyridine(s), thus enhancing the Lewis acidity of the nickel(II) center. As a result, reactivity of $\mathbf{1}^{[2]}$ and $\mathbf{1}^{[3]}$ toward H_2O_2 is enhanced to afford the bis(μ-oxo) complexes presumably through a LNi^{II}–OOH intermediate. Stability of the higher oxidation state of nickel(III) may also help the formation of the bis(μ-oxo)dinickel(III) complexes.

It should be also noted that the reactivity of the Ph_3tpa system is quite different between the nickel(II) and copper(II) complexes; the nickel(II) complex provided the bis(μ-oxo)-dinickel(III) complex $\mathbf{2}^{[3]}$, whereas the copper(II) complex was reduced to copper(I) (Scheme 1).[12] Such a big difference in reactivity in the Ph_3tpa sysetm can apparently be attributed to the difference in their redox potentials; $E_{1/2} = -0.82$ and -0.04 V vs. $Ag/AgNO_3$ for $[Ni^{II}(Ph_3tpa)(CH_3CN)](ClO_4)_2$ ($\mathbf{1}^{[3]}$) and $[Cu^{II}(Ph_3tpa)(CH_3CN)](ClO_4)_2$, respectively.[12] Namely, the reduced copper(I) complex is much more accessible than the nickel(I) complex, which is the reason why the copper(II) complex is easily reduced to the copper(I) complex.

Reactivity of the bis(μ-oxo)dinickel(III) complexes toward intramolecular ligand oxidation is also different from that of the bis(μ-oxo)dicopper(III) complex (Scheme 1); the bis(μ-oxo)-dinickel(III) complex induced the aromatic ligand hydroxylation at the *o*-position of 6-Ph via an electrophilic aromatic substitution mechanism (Figure 8), whereas the bis(μ-oxo)-dicopper(III) complex resulted in an oxidative *N*-dealkylation of the supporting ligand Ph_2tpa through a hydrogen atom abstraction and oxygen rebound mechanism or its concerted variant.[12] Thus, it becomes clear that the intrinsic reactivity of the bis(μ-oxo) complex between the nickel and copper systems are quite different. These results obtained in this study will provide significantly important insights into not only the substituent effects on the tpa-coordination chemistry but also the reactivity differences between the nickel and copper complexes supported by the same series of ligands.

This work was supported by Grant-in-Aid for Science Research on Priority Areas (No. 200360044, Synergy of Elements; No. 21108515, pi-Space) from Ministry of Education, Culture, Sports, Science and Technology, Japan. We also thank The Asahi Glass Foundation and The Mitsubishi Foundation for their financial supports.

Supporting Information

^{1}H NMR spectra of $\mathbf{1}^{[0]}$, $\mathbf{1}^{[1]}$, and $\mathbf{1}^{[3]}$ (Figures S1–S3) and cyclic voltammograms of $\mathbf{1}^{[1]}$, $\mathbf{1}^{[2]}$, and $\mathbf{1}^{[3]}$ (Figures S4–S6). This material is available free of charge on the Web at: http://www.csj.jp/journals/bcsj/.

References

1 a) L. M. Berreau, *Comments Inorg. Chem.* **2007**, *28*, 123. b) G. K. Ingle, R. W. Watkins, A. M. Arif, L. M. Berreau, *J. Coord. Chem.* **2008**, *61*, 61.

2 A. G. Blackman, *Eur. J. Inorg. Chem.* **2008**, 2633.

3 a) K. D. Karlin, S. Kaderli, A. D. Zuberbühler, *Acc. Chem. Res.* **1997**, *30*, 139. b) M.-A. Kope, K. D. Karlin, in *Biomimetic Oxidations Catalyzed by Transition Metal Complexes*, ed. by B. Meunier, Imperial College Press, London, **2000**, pp. 309–362. c) L. Q. Hatcher, K. D. Karlin, *J. Biol. Inorg. Chem.* **2004**, *9*, 669.

4 a) M. Costas, M. P. Mehn, M. P. Jensen, L. Que, Jr., *Chem. Rev.* **2004**, *104*, 939. b) X. Shan, L. Que, Jr., *J. Inorg. Biochem.* **2006**, *100*, 421. c) L. Que, Jr., *Acc. Chem. Res.* **2007**, *40*, 493.

5 M. Suzuki, *Acc. Chem. Res.* **2007**, *40*, 609.

6 S. Yamaguchi, H. Masuda, *Sci. Technol. Adv. Mater.* **2005**, *6*, 34.

7 E. Y. Tshuva, S. J. Lippard, *Chem. Rev.* **2004**, *104*, 987.

8 L. M. Mirica, X. Ottenwaelder, T. D. P. Stack, *Chem. Rev.* **2004**, *104*, 1013.

9 E. A. Lewis, W. B. Tolman, *Chem. Rev.* **2004**, *104*, 1047.

10 a) C.-L. Chuang, K. T. Lim, Q. Chen, J. Zubieta, J. W. Canary, *Inorg. Chem.* **1995**, *34*, 2562. b) C.-L. Chuang, K. Lim, J. W. Canary, *Supramol. Chem.* **1995**, *5*, 39.

11 D. Maiti, H. R. Lucas, A. A. N. Sarjeant, K. D. Karlin, *J. Am. Chem. Soc.* **2007**, *129*, 6998.

12 A. Kunishita, M. Kubo, H. Ishimaru, T. Ogura, H. Sugimoto, S. Itoh, *Inorg. Chem.* **2008**, *47*, 12032.

13 T. Fujii, A. Naito, S. Yamaguchi, A. Wada, Y. Funahashi, K. Jitsukawa, S. Nagatomo, T. Kitagawa, H. Masuda, *Chem. Commun.* **2003**, 2700.

14 a) S. Hikichi, M. Yoshizawa, Y. Sasakura, M. Akita, Y. Moro-oka, *J. Am. Chem. Soc.* **1998**, *120*, 10567. b) S. Itoh, H. Bandoh, S. Nagatomo, T. Kitagawa, S. Fukuzumi, *J. Am. Chem. Soc.* **1999**, *121*, 8945. c) K. Shiren, S. Ogo, S. Fujinami, H. Hayashi, M. Suzuki, A. Uehara, Y. Watanabe, Y. Moro-oka, *J. Am. Chem. Soc.* **2000**, *122*, 254. d) B. S. Mandimutsira, J. L. Yamarik, T. C. Brunold, W. Gu, S. P. Cramer, C. G. Riordan, *J. Am. Chem. Soc.* **2001**, *123*, 9194. e) S. Itoh, H. Bandoh, M. Nakagawa, S. Nagatomo, T. Kitagawa, K. D. Karlin, S. Fukuzumi, *J. Am. Chem. Soc.* **2001**, *123*, 11168. f) R. Schenker, B. S. Mandimutsira, C. G. Riordan, T. C. Brunold, *J. Am. Chem. Soc.* **2002**, *124*, 13842.

15 S. Yao, E. Bill, C. Milsmann, K. Wieghardt, M. Driess, *Angew. Chem., Int. Ed.* **2008**, *47*, 7110.

16 a) K. Fujita, R. Schenker, W. Gu, T. C. Brunold, S. P. Cramer, C. G. Riordan, *Inorg. Chem.* **2004**, *43*, 3324. b) M. T. Kieber-Emmons, R. Schenker, G. P. A. Yap, T. C. Brunold, C. G. Riordan, *Angew. Chem., Int. Ed.* **2004**, *43*, 6716. c) R. Schenker, M. T. Kieber-Emmons, C. G. Riordan, T. C. Brunold, *Inorg. Chem.* **2005**, *44*, 1752.

17 a) M. T. Kieber-Emmons, J. Annaraj, M. S. Seo, K. M. V. Heuvelen, T. Tosha, T. Kitagawa, T. C. Brunold, W. Nam, C. G.

Riordan, *J. Am. Chem. Soc.* **2006**, *128*, 14230. b) J. Cho, R. Sarangi, J. Annaraj, S. Y. Kim, M. Kubo, T. Ogura, E. I. Solomon, W. Nam, *Nat. Chem.* **2009**, *1*, 568.

18 S. Hikichi, H. Okuda, Y. Ohzu, M. Akita, *Angew. Chem., Int. Ed.* **2009**, *48*, 188.

19 W. L. F. Armarego, D. D. Perrin, *Purification of Laboratory Chemicals*, 4th ed., Butterworth-Heinemann, Oxford, **1996**.

20 Z. Tyeklár, R. R. Jacobson, N. Wei, N. N. Murthy, J. Zubieta, K. D. Karlin, *J. Am. Chem. Soc.* **1993**, *115*, 2677.

21 M. P. Jensen, E. L. Que, X. Shan, E. Rybak-Akimova, L. Que, Jr., *Dalton Trans.* **2006**, 3523.

22 M. M. Makowska-Grzyska, E. Szajna, C. Shipley, A. M. Arif, M. H. Mitchell, J. A. Halfen, L. M. Berreau, *Inorg. Chem.* **2003**, *42*, 7472.

23 M. Ito, K. Sakai, T. Tsubomura, Y. Takita, *Bull. Chem. Soc. Jpn.* **1999**, *72*, 239.

24 SIR92: A. Altomare, G. Cascarano, C. Giacovazzo, A. Guagliardi, M. C. Burla, G. Polidori, M. Camalli, *J. Appl. Crystallogr.* **1994**, *27*, 435.

25 Crystal Structure: *Crystal Structure Analysis Package version 3.8.1*, Molecular Structure Corp. and Rigaku Corp., **2005**.

26 E. Szajna, P. Dobrowolski, A. L. Fuller, A. M. Arif, L. M. Berreau, *Inorg. Chem.* **2004**, *43*, 3988.

27 L. Que, Jr., W. B. Tolman, *Angew. Chem., Int. Ed.* **2002**, *41*, 1114.

28 Since the bis(μ-oxo)dinickel(III) complex $\mathbf{2}^{[2]}$–^{16}O was generated in situ by adding a diluted $H_2{}^{16}O_2$ aqueous solution ($H_2{}^{16}O$) to $\mathbf{1}^{[2]}$, $^{16}O/^{18}O$ isotope exchange experiment by adding $H_2{}^{18}O$ to a solution of $\mathbf{2}^{[2]}$–^{16}O containing a large excess of $H_2{}^{16}O$ was unsuccessful.

29 A. Kunishita, Y. Doi, M. Kubo, T. Ogura, H. Sugimoto, S. Itoh, *Inorg. Chem.* **2009**, *48*, 4997.

30 K. Honda, J. Cho, T. Matsumoto, J. Roh, H. Furutachi, T. Tosha, M. Kubo, S. Fujinami, T. Ogura, T. Kitagawa, M. Suzuki, *Angew. Chem., Int. Ed.* **2009**, *48*, 3304.

31 S. Itoh, *Curr. Opin. Chem. Biol.* **2006**, *10*, 115.